SAND2018-13655PE

Characterization of Neutron Diagnostics at the Ion Beam Laboratory for Inertial Confinement Fusion Applications

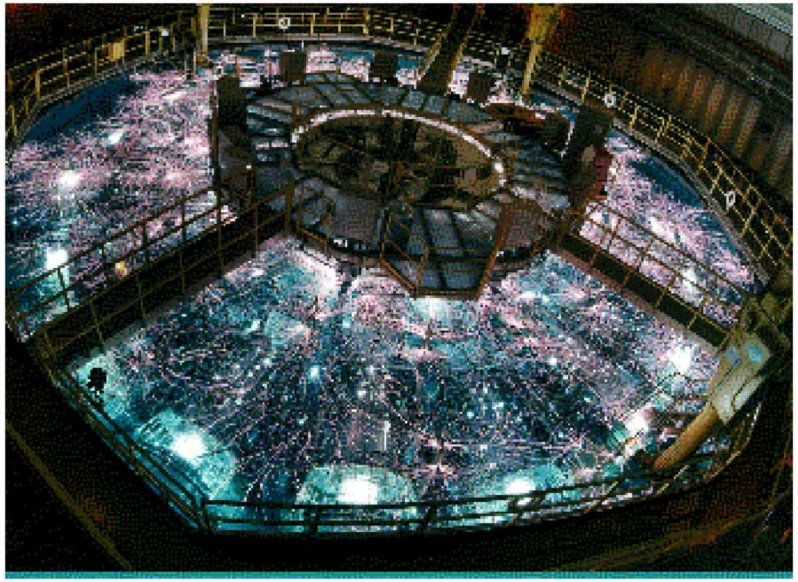

Jedediah Styron, Research Faculty
Dept. of Nuclear Engineering
University of New Mexico

National Diagnostic Working Group Meeting
December 6, 2018
Rochester, NY

Sandia National Laboratories is a multimission laboratory managed and operated by National Technology and Engineering Solutions of Sandia, LLC., a wholly owned subsidiary of Honeywell International, Inc., for the U.S. Department of Energy's National Nuclear Security Administration under contract DE-NA-0003525.

Collaborators

- University of New Mexico
  - Gary Cooper
  - Sara Pelka
  - Jeremy Vaughan
  - Colin Weaver
- Lawrence Livermore National Laboratories
  - Kelly Hahn
  - Christopher Cooper
  - James Mitrani
- National Nuclear Security Site
  - Ken Moy
  - Robert Buckles
- Sandia National Laboratories
  - Carlos Ruiz
  - Gordon Chandler
  - Bill Wampler
  - Ed Bielejec
  - Bruce McWatters
  - Jose Torres
  - Brent Jones
  - Clark Highstrete
  - Barney Doyle

Summary

- The Ion Beam Laboratory at Sandia National Laboratories is an invaluable facility that supports many scientific campaigns
- Neutrons produced at the IBL are known absolutely to < 7% using the Associated Particle Method.
- The experimental geometry at the IBL has a complete diagnostic infrastructure in place and is flexible in the test diagnostics that can be supported.
- Two new end stations are being developed
  - High precision test chamber
  - High fluence DT neutron irradiations
- IBL is a user friendly facility that has produced successful collaborations external to SNL.

Outline

- Introduction to the IBL facility
- Inference of the neutron yield and energy
- Diagnostic characterization
    - Passive activation samples
    - In-situ activation detectors
    - CR39 track detectors
    - Time-of-flight
- Future capabilities
    - Improved diagnostic chambers
    - High fluence test station

Sandia’s Ion Beam Laboratory (IBL)

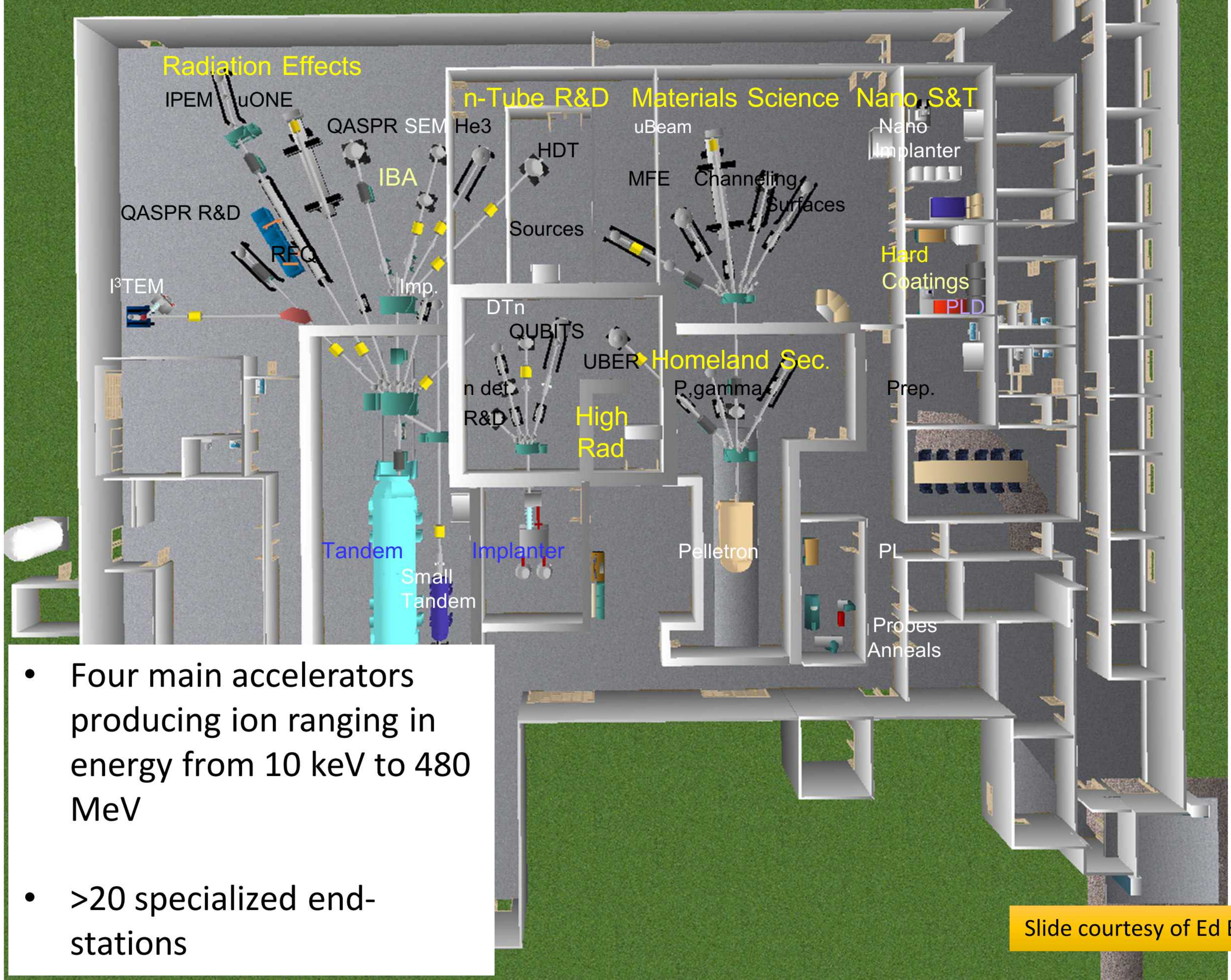

- Four main accelerators producing ion ranging in energy from 10 keV to 480 MeV
- >20 specialized end-stations

Slide courtesy of Ed Bielejec, IBL Manager

Neutron diagnostics are characterized using the neutron calibration chamber (NUCAL) at the Ion Beam Laboratory (IBL).

- Ion beam generated using a 350 keV Cockroft-Walton HVEE accelerator
  - Magnetically analyzed beam
  - Electrostatic focusing
  - Electromagnetic steering
  - Pulse beam or steady state (ms – days)

- Target chamber
  - Adjustable sample holder
  - 7.6 – 33.0 cm at 0 to -180 degrees with respect to the beam
  - Rotating target with water or air cooling

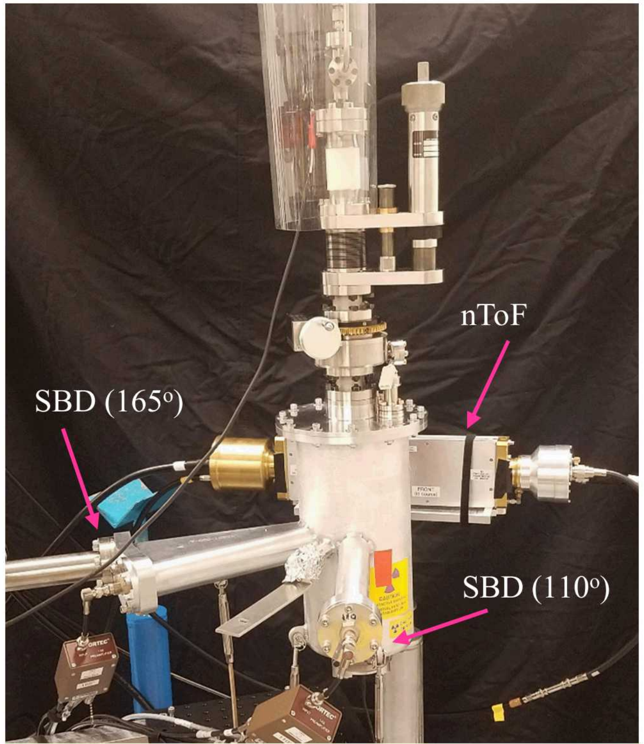

NUCAL target chamber, shown with a dual PMT nToF under study

C. L. Ruiz et al., Rev. Sci. Instrum. **83**, 10D913 (2012)

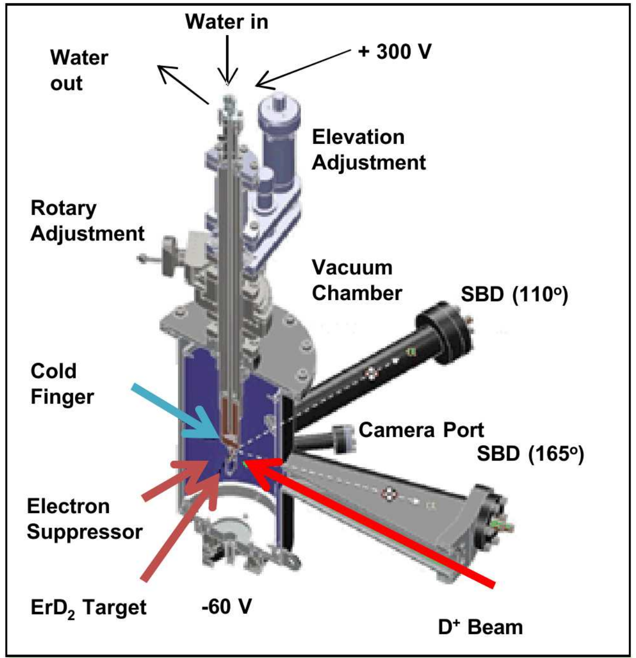

Schematic of the NUCAL target chamber

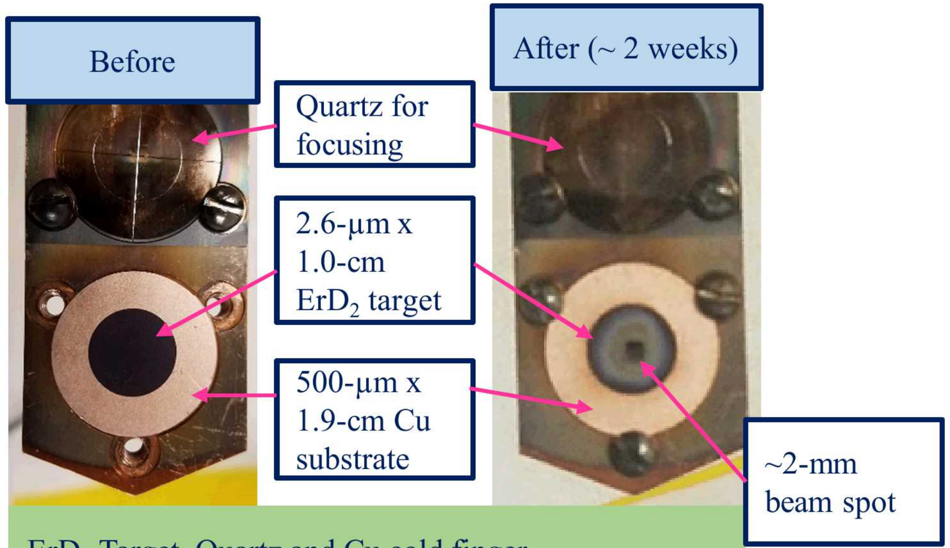

ErD_2 Target, Quartz and Cu cold finger

The neutron yield per steradian at any angle is inferred using the Associated Particle Method (APM).

- Associated Particle Method
  - Transformation of differential cross-sections from center-of-mass to the lab frame using relativistic kinematics
  - Accounts for loading ratio and dE/dx ion losses in the target

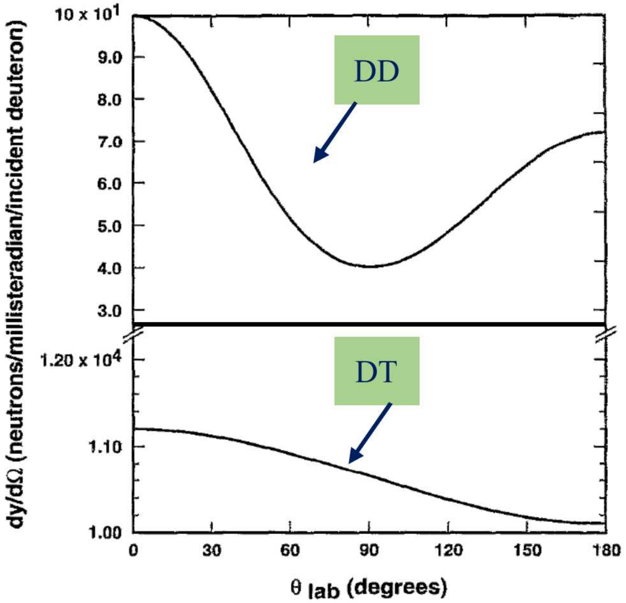

Estimated thick target neutron yield for DD and DT reactions as a function of lab angle

Thick target yield

$$\frac{dy}{d\Omega} = \int_{E_{max}}^{0} \frac{n\,d\sigma(E)/d\Omega}{dE/dx}\,dE$$

Loading ratio

D+ stopping power

Incident neutron fluence on a cylindrical sample

$$\phi\left[\frac{n}{cm^2}\right] = (C - B)_\alpha \left(\frac{Y_n}{Y_\alpha}\right)\left(\frac{\Omega_n}{\Omega_\alpha}\right)\left(\frac{t_o}{\pi r_s^2}\right)$$

Neutron flux

Net Charged Particle Counts

Calculated yield ratio

Solid angle ratio

Sample surface area

Irradiation time

C. L. Ruiz et al., Rev. Sci. Instrum., **63**, 4889 (1992)
C. L. Ruiz et al., Rev. Sci. Instrum. **83**, 10D913 (2012)

The calibration factor inferred for the activation diagnostics is known as the F-factor.

- F-factor characterizes the entire detector system
- Examples:
  - Indium sample + HPGe detector
  - Copper sample + NaI coincidence
  - Beryllium detector + CFD (constant fraction discriminator)

Expected number of net counts from an exposed cylindrical activation sample

$$(C-B)_n = \frac{\phi\varepsilon_A\varepsilon_D\varepsilon_S\varepsilon_B M N_A \sigma(E)\left[\left(1-\mathrm{e}^{\lambda t_o}\right)\left(e^{-\lambda t_1}-e^{-\lambda t_2}\right)\right]}{\lambda A_w}$$

Calibration F-factor

$$F\left[\left(\frac{cts}{n}\right)\left(\frac{cm^2}{g}\right)\right] = \frac{\phi\varepsilon_A\varepsilon_D\varepsilon_S\varepsilon_B N_A \sigma(E)}{\lambda A_w}$$

F-Factor as determined from measurable quantities at IBL

$$F\left[\left(\frac{cts}{n}\right)\left(\frac{cm^2}{g}\right)\right] = \frac{\lambda(C-B)_n}{\phi M\left[\left(1-\mathrm{e}^{\lambda t_o}\right)\left(e^{-\lambda t_1}-e^{-\lambda t_2}\right)\right]}$$

Isotropic neutron yield as calculated for a MagLIF experiment (Implementing the F-Factor)

$$Y_z = 4\pi d^2\phi(d) = \frac{4\pi d^2(C-B)_z}{FM\left(e^{-\lambda t_1}-e^{-\lambda t_2}\right)}$$

C. L. Ruiz et al., Rev. Sci. Instrum., **63**, 4889 (1992)
C. L. Ruiz et al., Rev. Sci. Instrum. **83**, 10D913 (2012)
J. D. Styron et al., Rev. Sci. Instrum. **85**, 11E617 (2014)
C. L. Ruiz et al., submitted to Physical Review Special Topics (2018)

Activation samples are irradiated under steady state conditions, removed, and counted ex-situ.

Indium Activation (D-D)

$^{115}\text{In}(n,\gamma)^{115m}\text{In} \rightarrow 336\ \text{keV}\ \gamma \rightarrow {}^{115}\text{In}$

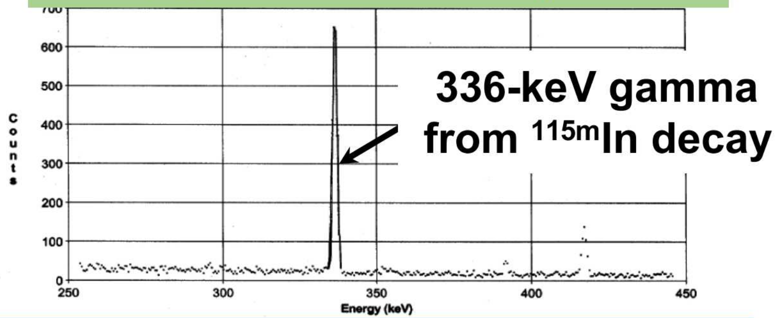

The indium activation spectrum is measured using high-purity germanium detectors.

Copper
(0.95 X 7.62 cm)

Indium
(1.24 X 2.54 cm)

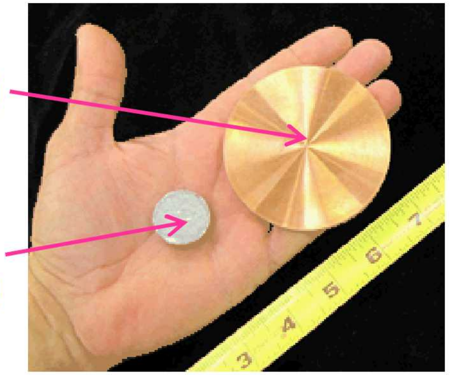

Copper Activation (D-T)

$^{63}\text{Cu}(n,2n)^{62}\text{Cu} \rightarrow 1.32\ \text{MeV}\ \beta^{+} \rightarrow {}^{62}\text{Ni}\ (100\%)$

$^{65}\text{Cu}(n,2n)^{64}\text{Cu} \rightarrow 0.65\ \text{MeV}\ \beta^{+} \rightarrow {}^{64}\text{Ni}\ (61\%)$

Copper activity is inferred by measuring the 511-keV annihilation gamma’s in coincidence.

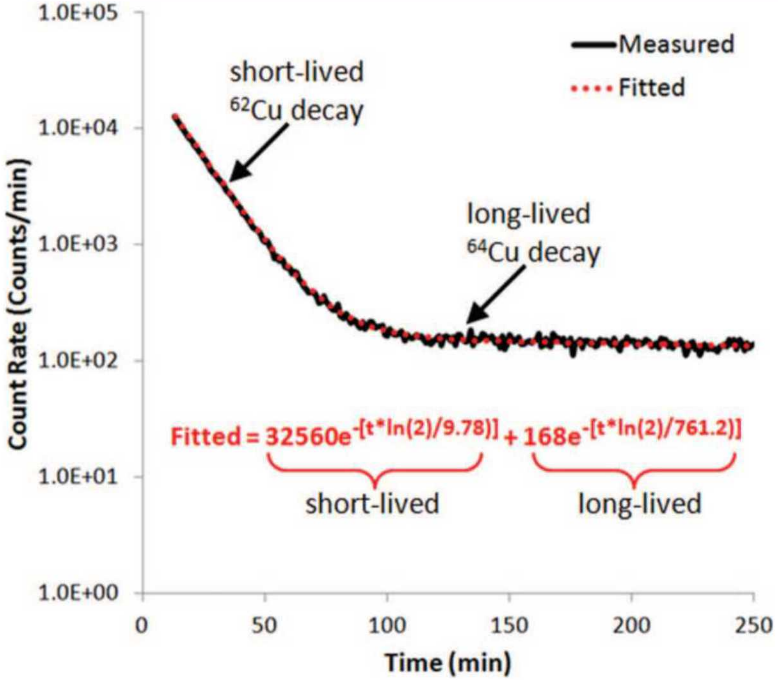

C. L. Ruiz et al., Rev. Sci. Instrum., **63**, 4889 (1992)
K. D. Hahn et al., Rev. Sci. Instrum., **83**, 10D914 (2012)
K. D. Hahn et al., Rev. Sci. Instrum., **85**, 043507 (2014)
K.D. Hahn et al., J. Appl. Phys., **717**, 012020 (2016)

A pulse irradiation scheme has been included on the HVEE accelerator to characterize in-situ activation detectors.

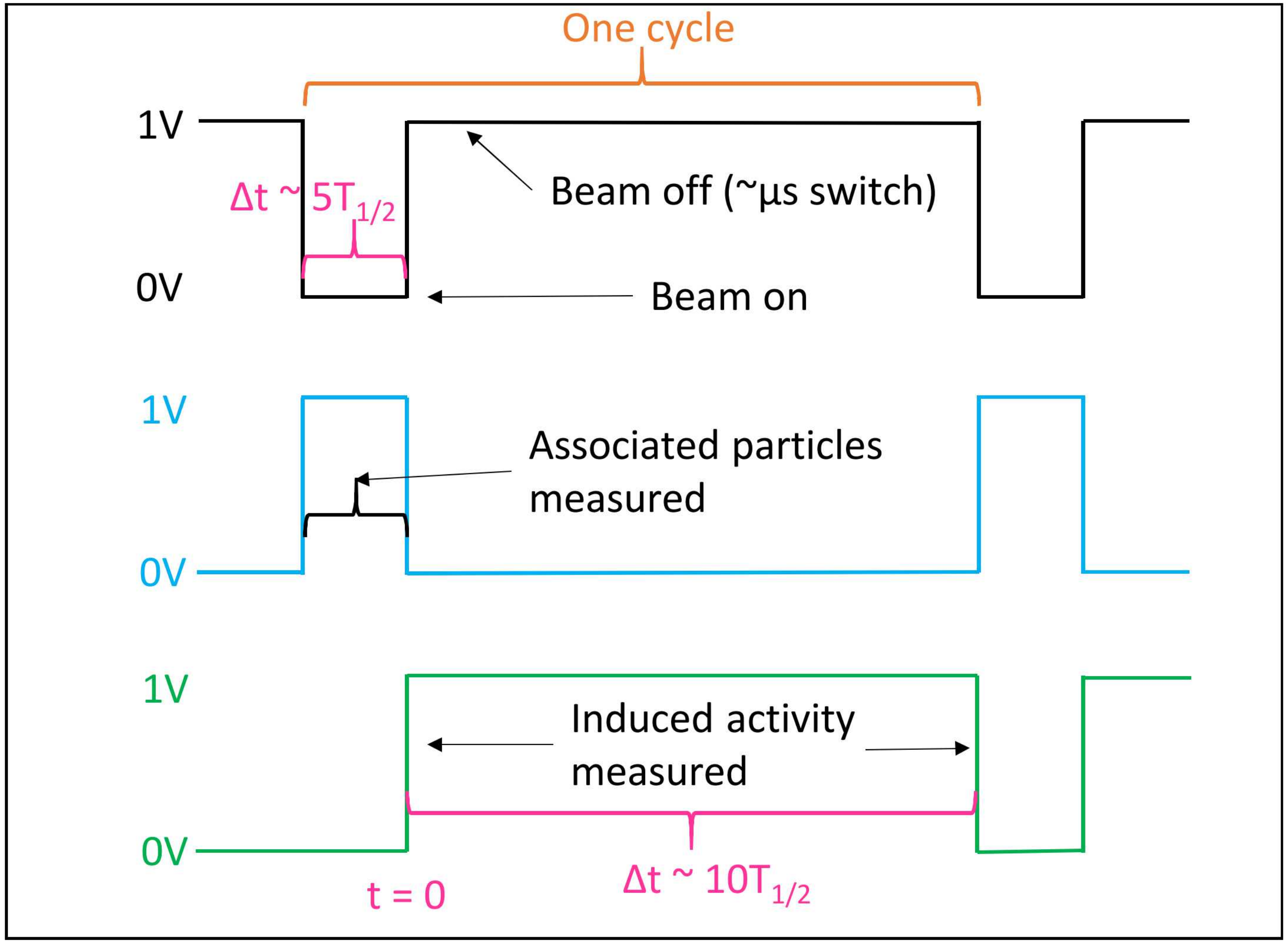

- Pulse scheme is controlled using a delay generator
  - Delay generator controls beam deflector
  - Associated particles are inferred when the beam is on target
  - Induced activity is measured when beam is off target
  - Number of cycles are chosen to produce favorable counting statistics
  - Cycle times are chosen based on the half-life of the desired isotope.

Groups at SNL and LLNL have used the pulse beam to compare F-factors for nearly identical Be-activation detectors.

Be-activation detector (D-D)

$^9\text{Be}(n,\alpha)^6\text{He} \rightarrow 3.51$ MeV $\beta^- \rightarrow {}^6\text{Li}$

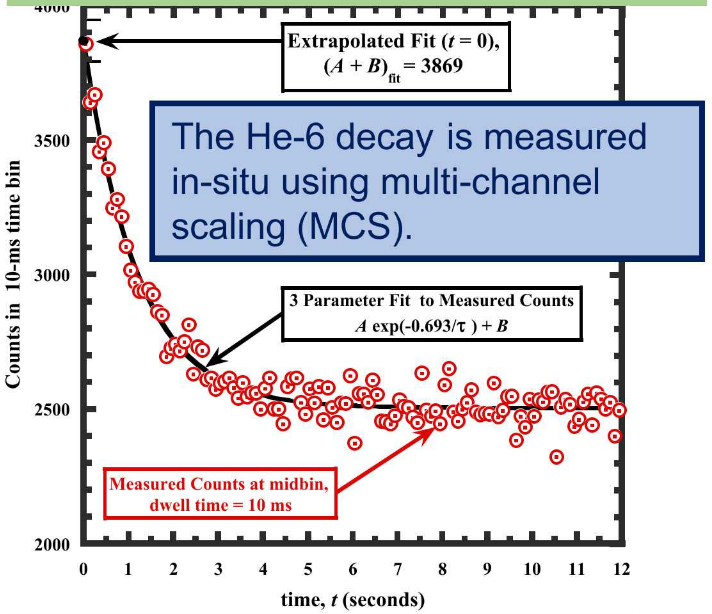
The He-6 decay is measured in-situ using multi-channel scaling (MCS).

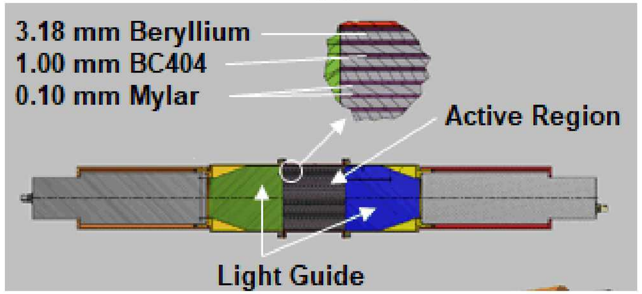

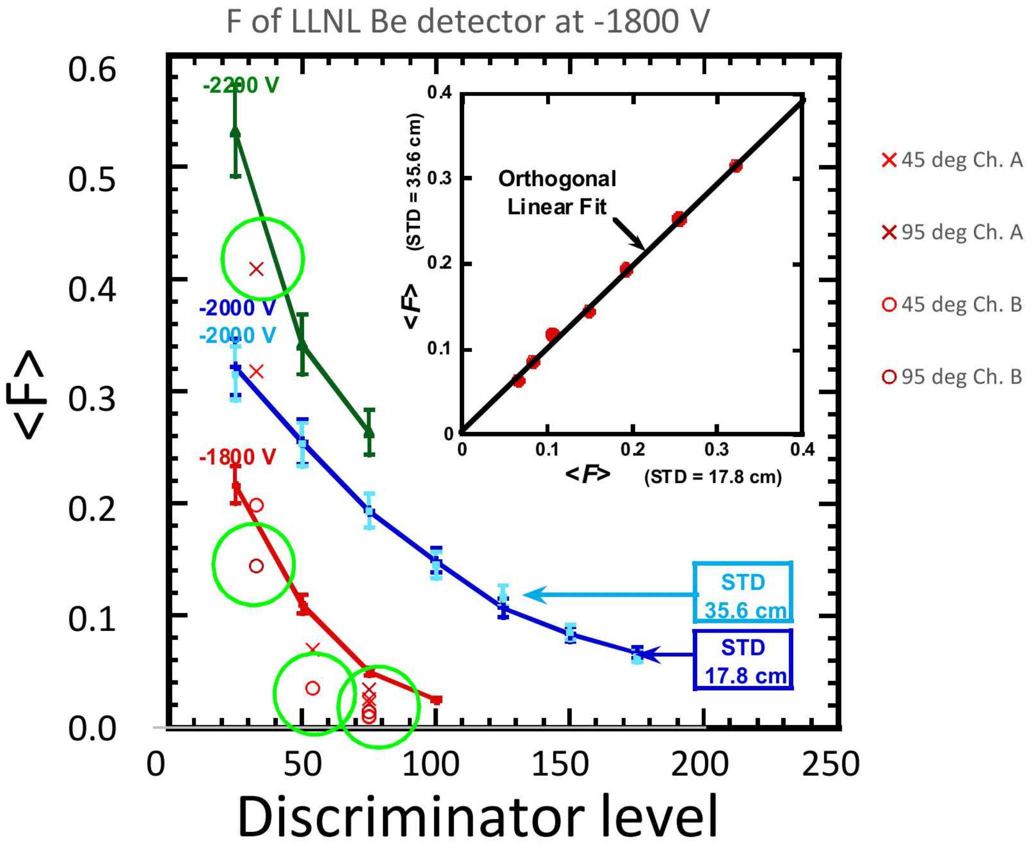

Data courtesy of James Mitrani, LLNL

SNL fields two Be detectors on Z as a primary yield diagnostic

LLNL is using there Be detector to characterize a new MJ class DPF

Cals at 45 degrees are higher than at 95 degrees due to higher flux, cross section, and energy

LLNL calibrations in green

LLNL has developed a LaBr3(Ce) detector that has been characterized at the IBL using a pulsed beam

Alignment of the $LaBr_3$ detector at 95° with respect to the ion beam

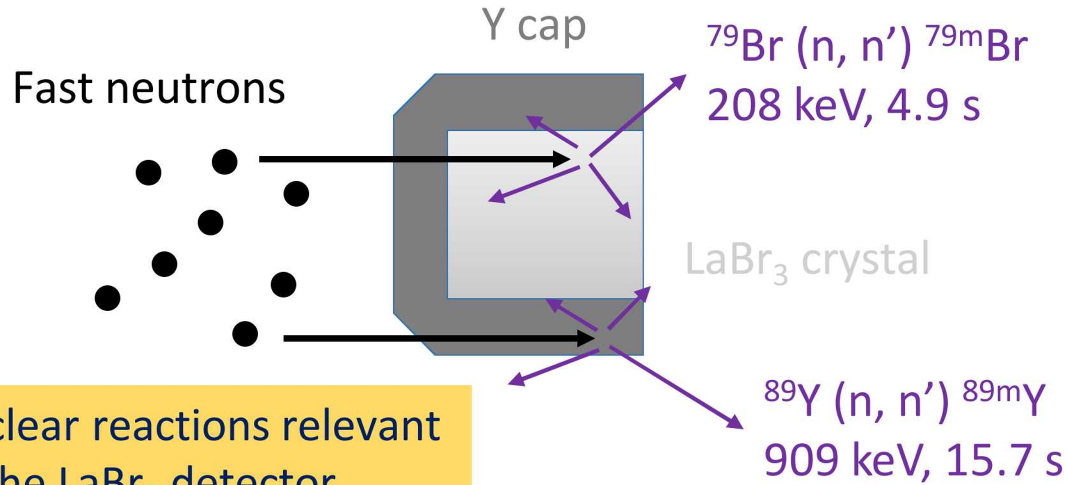

Y cap

Fast neutrons

$^{79}Br\ (n, n')\ ^{79m}Br$
208 keV, 4.9 s

$LaBr_3$ crystal

$^{89}Y\ (n, n')\ ^{89m}Y$
909 keV, 15.7 s

Nuclear reactions relevant to the $LaBr_3$ detector

In-situ gamma spectroscopy

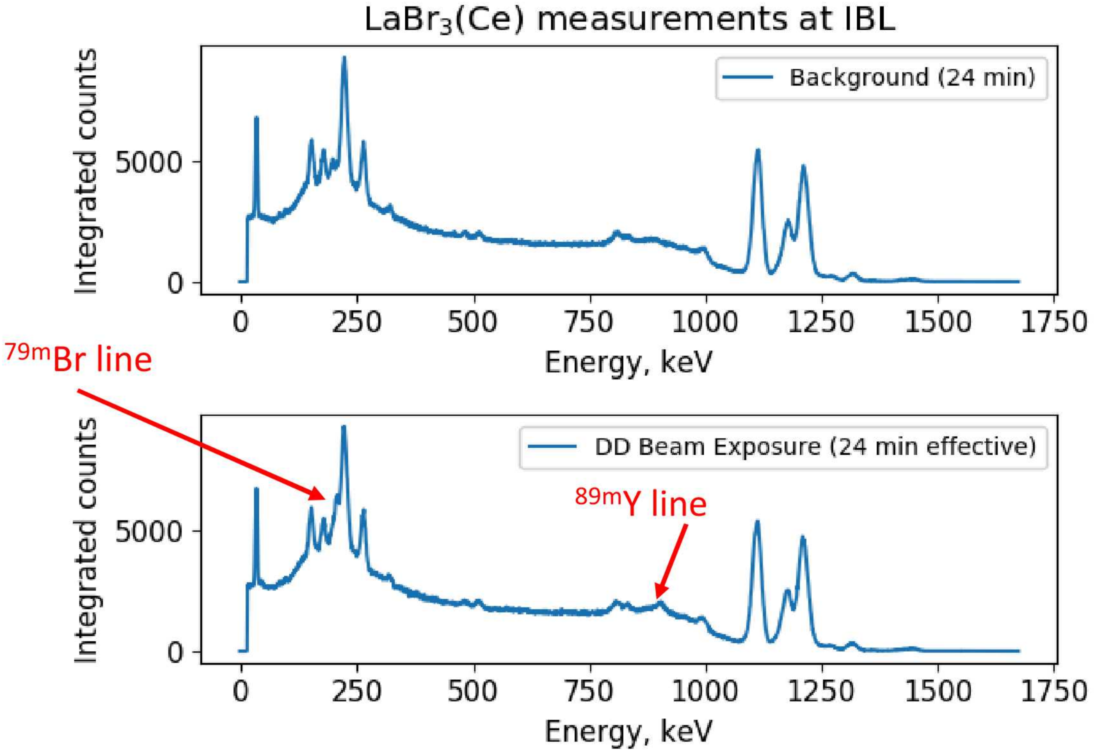

Data courtesy of James Mitrani, LLNL

A CR39 based One Dimensional Imager of Neutrons is being tested at the IBL to understand the point spread function of the slit and the efficiencies of different radiator materials.

J. Frenje et al., Rev. Sci. Instr. **73,** 2597 (2002)
D. Ampleford et al. (accepted by Rev. Sci. Instr. **89** (2018)
J. Vaughan et al. (accepted by Rev. Sci. Instr. **89** (2018)

- CR-39 is a plastic substrate used to measure charged particles
- Etched with a 6-mol NaOH solution and viewed under a microscope to view the particle tracks

Experimental Results using the sample shown below at two different distances

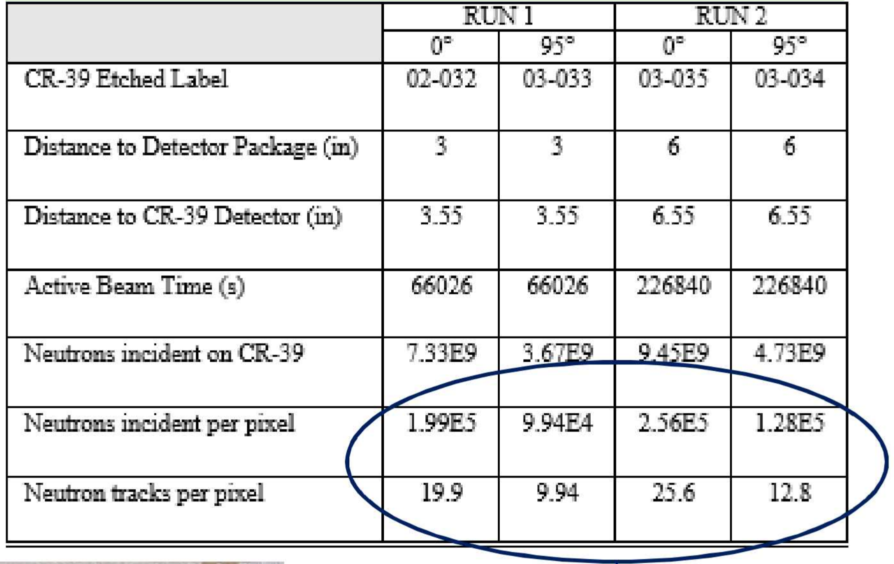

	RUN 1		RUN 2	
	0°	95°	0°	95°
CR-39 Etched Label	02-032	03-033	03-035	03-034
Distance to Detector Package (in)	3	3	6	6
Distance to CR-39 Detector (in)	3.55	3.55	6.55	6.55
Active Beam Time (s)	66026	66026	226840	226840
Neutrons incident on CR-39	7.33E9	3.67E9	9.45E9	4.73E9
Neutrons incident per pixel	1.99E5	9.94E4	2.56E5	1.28E5
Neutron tracks per pixel	19.9	9.94	25.6	12.8

DT neutron efficiency is 1E-4

(tracks/incident neutron)

Typical scan of a CR-39 sample

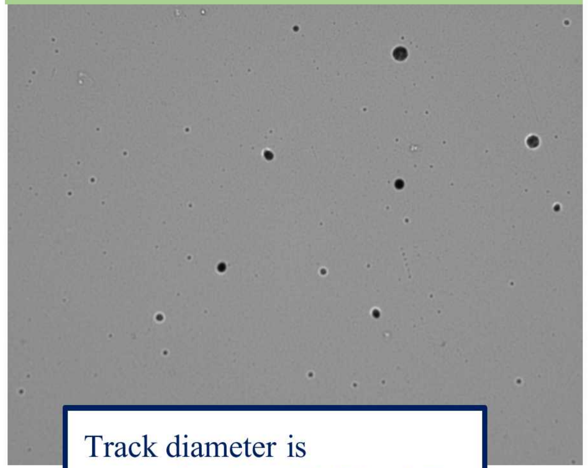

Track diameter is proportional to dE/dX ~ 1/E

CR-39 samples (shown to the right) fielded at the IBL and exposed to DT neutrons

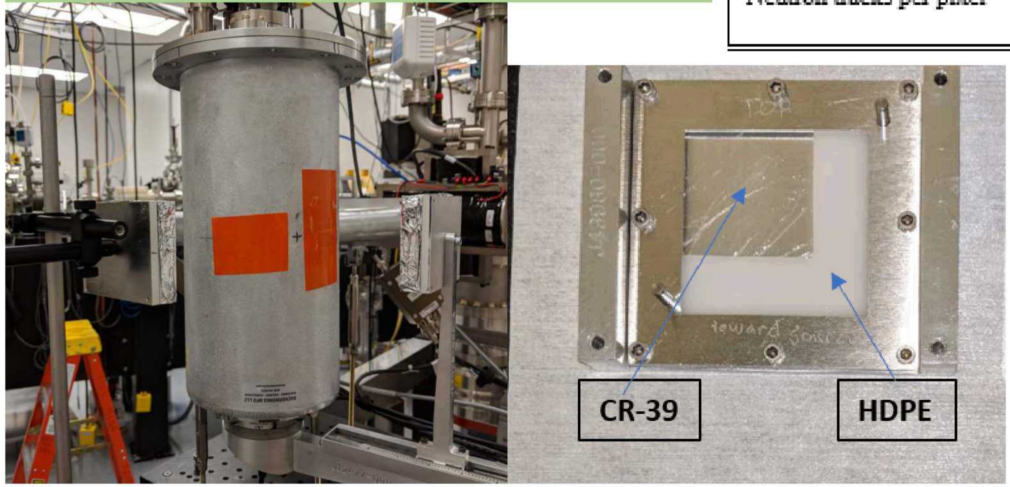

A special thanks to M. Gatu Johnson and Brandon Lahman for helping out with the scanning and processing of the CR39!

Particle coincidence is derived from the reaction kinematics and used to infer the nToF detector instrument response function to single DT or DD neutron interactions.

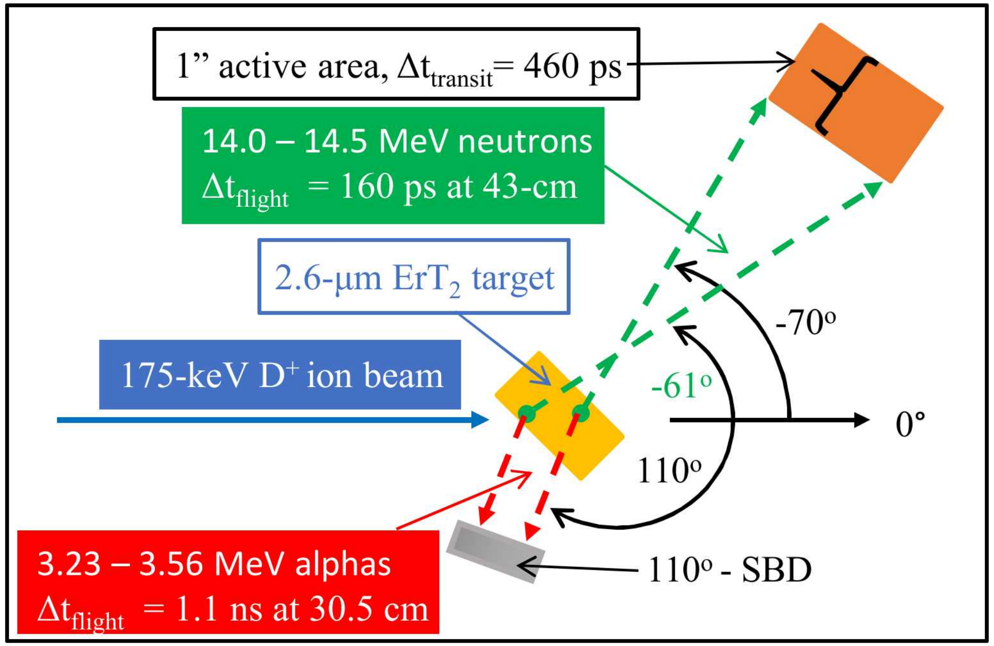

1” active area, $\Delta t_{transit}$= 460 ps

14.0 – 14.5 MeV neutrons
Δt_{flight} = 160 ps at 43-cm

2.6-µm ErT_2 target

175-keV D^+ ion beam

-70°

-61°

0°

110°

110° - SBD

3.23 – 3.56 MeV alphas
Δt_{flight} = 1.1 ns at 30.5 cm

Kinematic relationship for an alpha particle emitted into an angle of 110-degrees

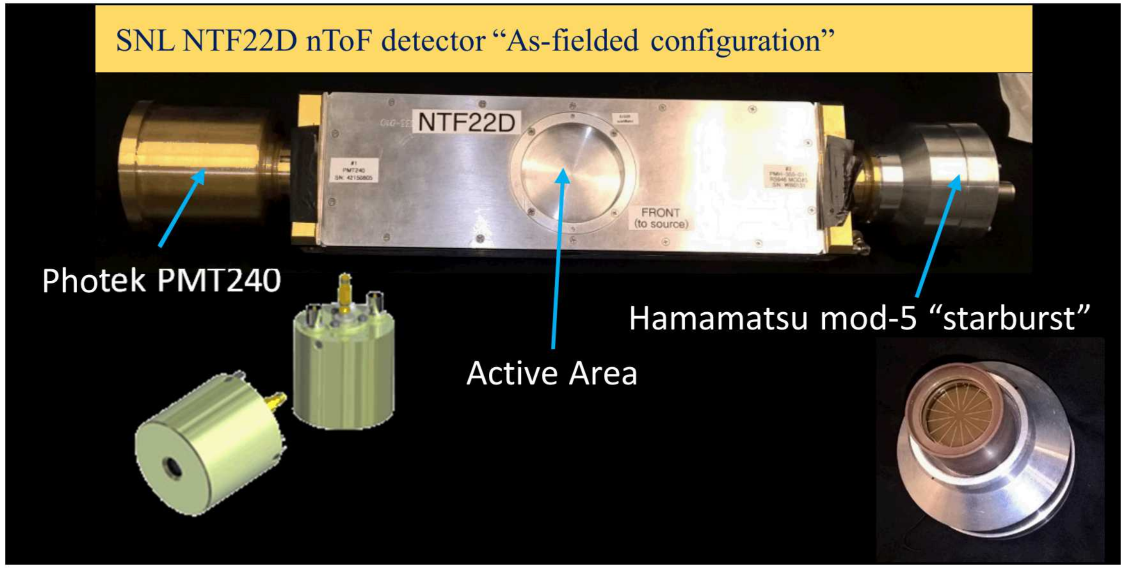

SNL NTF22D nToF detector “As-fielded configuration”

Photek PMT240

Active Area

Hamamatsu mod-5 “starburst”

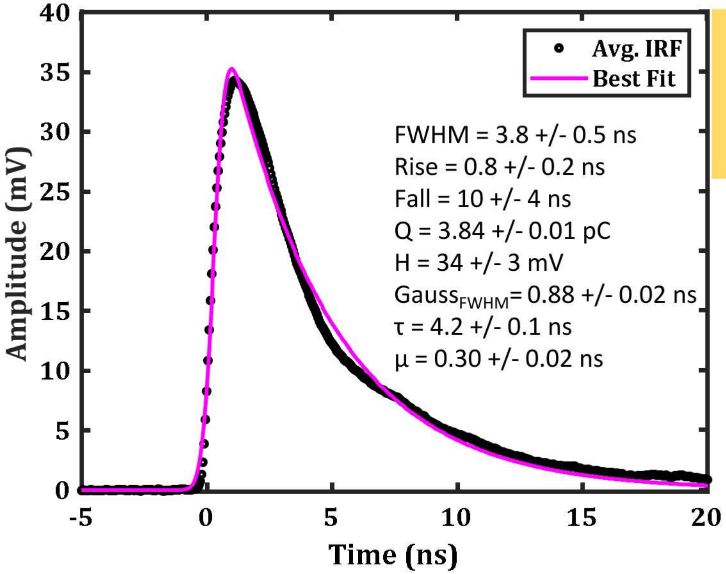

FWHM = 3.8 +/- 0.5 ns
Rise = 0.8 +/- 0.2 ns
Fall = 10 +/- 4 ns
Q = 3.84 +/- 0.01 pC
H = 34 +/- 3 mV
$Gauss_{FWHM}$= 0.88 +/- 0.02 ns
τ = 4.2 +/- 0.1 ns
µ = 0.30 +/- 0.02 ns

Representative instrument response function. Data shown for detector NTF22D-Photek PMT240 at -4.0 kV w/ EJ228 scintillator

A new chamber is in conceptual development to further enhance our calibration capabilities .

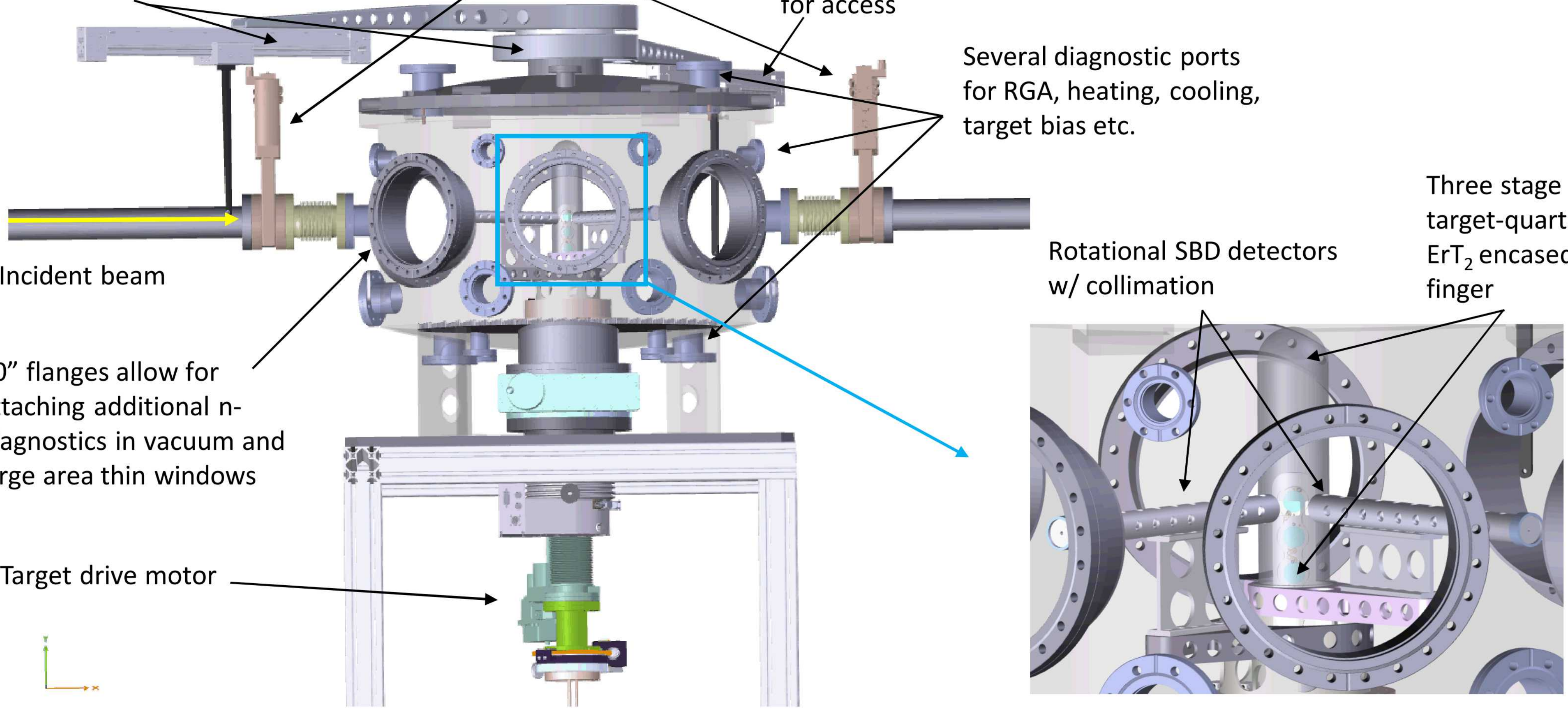

Two sample holders with precision settings for distance and angle.

Chamber isolation valves

Top plate is hinged for access

Several diagnostic ports for RGA, heating, cooling, target bias etc.

Incident beam

Three stage rotational target-quartz, ErD$_2$, and ErT$_2$ encased in a cold finger

Rotational SBD detectors w/ collimation

10” flanges allow for attaching additional n-diagnostics in vacuum and large area thin windows

Target drive motor

14 MeV Neutrons for Radiation Effects Testing at the Sandia Ion Beam Lab

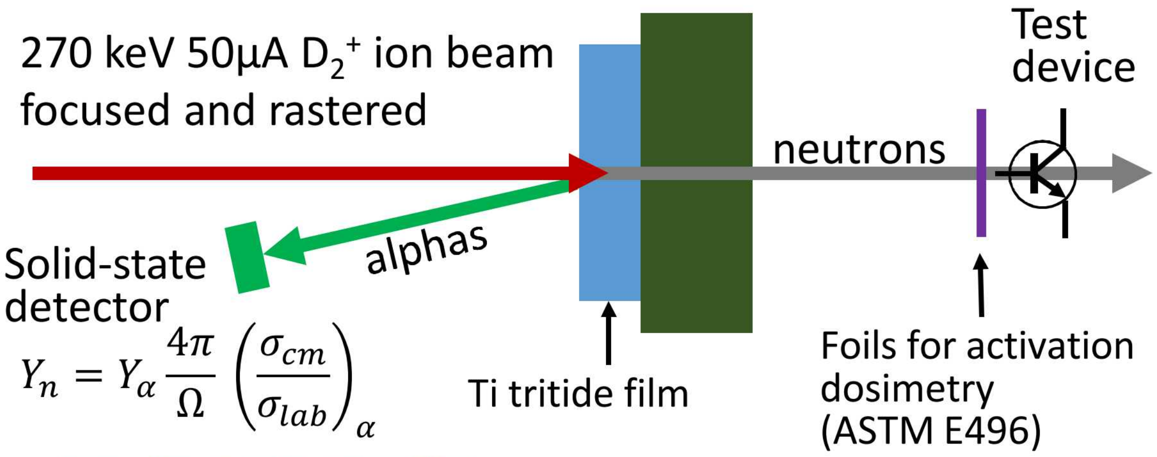

270 keV 50µA D_2^+ ion beam focused and rastered

neutrons

Test device

alphas

Solid-state detector

Ti tritide film

Foils for activation dosimetry (ASTM E496)

$$Y_n = Y_\alpha \frac{4\pi}{\Omega}\left(\frac{\sigma_{cm}}{\sigma_{lab}}\right)_\alpha$$

Neutron production rate determined by:

1. α yield (real-time)
2. Dosimetry foil activity (Total fluence)
3. D beam current & reaction cross section (initial value)

All agree

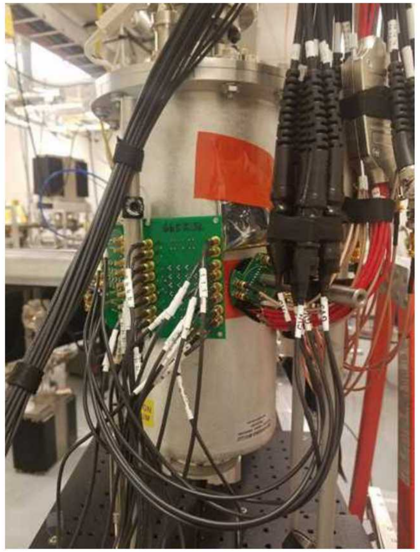

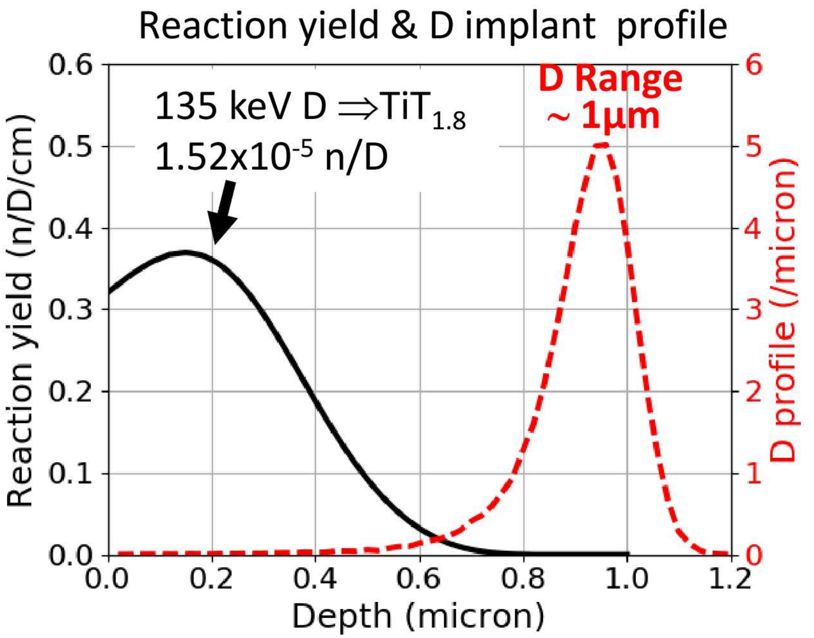

At test location outside target chamber (R=7.6 cm)

Initial neutron flux ~ 1.5x10^7 n/cm^2/s

Total n fluence from a target ~ 3.4x10^{12} n/cm^2

Slide courtesy of W. Wampler

Neutron production rate decreases with time due to tritium loss from target by isotope exchange.

Slide courtesy of W. Wampler

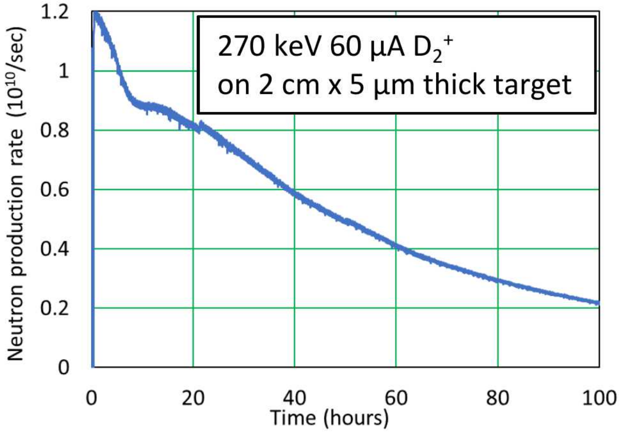

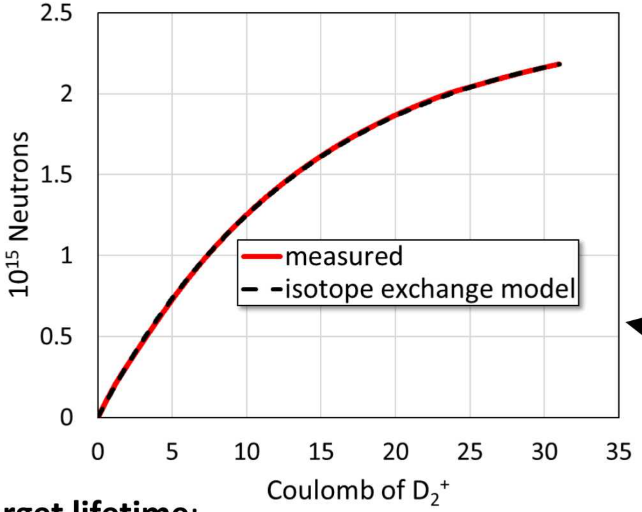

Target lifetime:
N = 1.6×10^{20} atoms of T in target initially
$q_eN/2$ = 13 Coulomb D_2^+ target lifetime
= 60 hours at 60 µA
σ N = 2.4×10^{15} neutrons per target

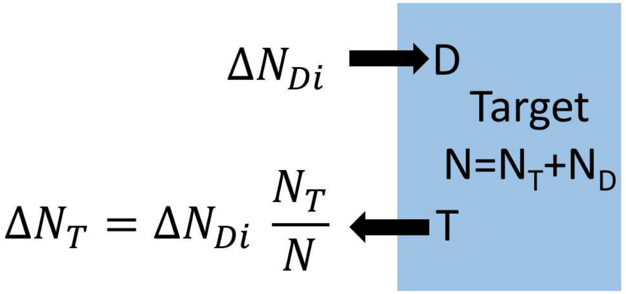

$$\Delta N_{Di}$$

$$\Delta N_T = \Delta N_{Di} \frac{N_T}{N}$$

- Implanted D mixes with T in target.
- Total number of D+T atoms in target is constant determined by stoichiometry and film volume. Remaining tritium:

$$N_T = N\, exp\left(-\frac{N_{Di}}{N}\right)$$

- Number of neutrons produced per incident D:

$$\frac{dN_n}{dN_{Di}} = \sigma \frac{N_T}{N} = \sigma\, exp\left(-\frac{N_{Di}}{N}\right)$$

- Number of neutrons produced:

$$N_n = \sigma\, N \left(1 - exp\left(-\frac{N_{Di}}{N}\right)\right)$$

Number of neutrons per target and target lifetime are determined by the amount of tritium undergoing exchange, i.e. area and thickness of tritide film.

New beamline/test chamber for higher fluence

Slide courtesy of W. Wampler

A new beamline and target chamber optimized for testing effects of 14 MeV neutrons on electronics is being constructed.
Neutron flux & fluence at test location increased ~50x to $>10^{14}/\text{cm}^2$ per target by decreasing distance from source to test location from 7.6 to 1 cm.

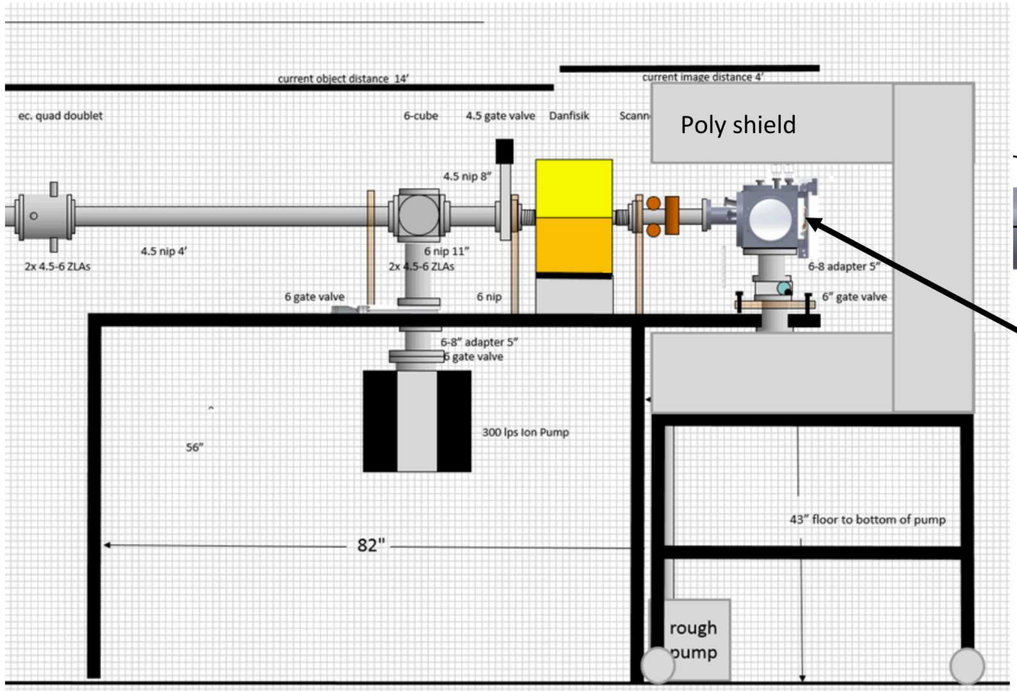

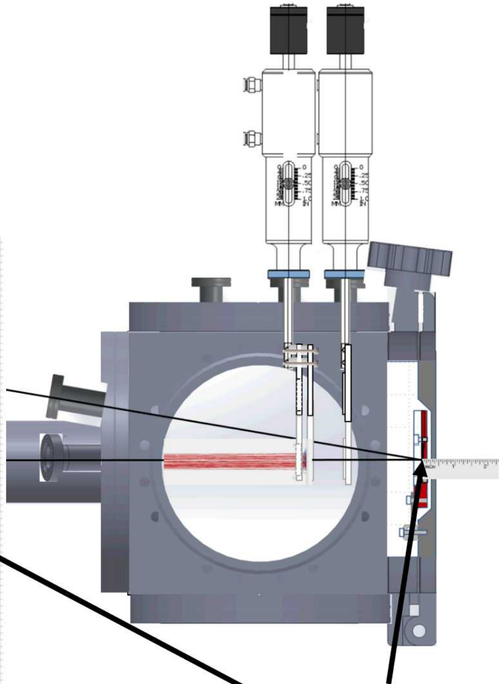

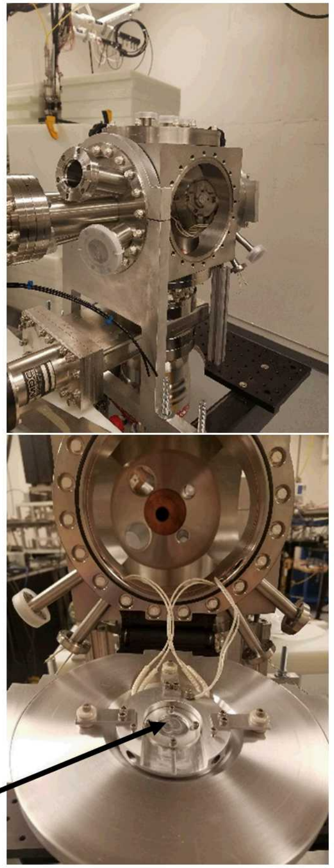

target

Summary

- The Ion Beam Laboratory at Sandia National Laboratories is an invaluable facility that supports many scientific campaigns
- Neutrons produced at the IBL are known absolutely to < 7% using the Associated Particle Method.
- The experimental geometry at the IBL has a complete diagnostic infrastructure in place and is flexible in the test diagnostics that can be supported.
- Two new end stations are being developed
  - High precision test chamber
  - High fluence DT neutron irradiations
- IBL is a user friendly facility that has produced successful collaborations external to SNL.

Back-up slides

S.A. Slutz et al., Phys. of Plasma,**17**, 056303(2010)
A.B. Sefkow et al., Phys. of Plasma,**21**, 072711 (2014)
M.R. Gomez et al., Phys. Rev. Lett. **113**, 155003 (2014)

The MagLIF (Magnetized Liner Inertial Fusion) concept is being developed as a fusion source at the Z-accelerator.

- Deuterium gas load, 0.7 mg/cm^3 at 60 psi
- External magnetization ~ 10 Tesla
- Laser Pre-heat ~ 2.5 kJ
- Beryllium liner compression ~ 20 MA
- 2-3 keV ion temperatures
- 3E12 D-D neutron yield

Primary Reactions

$$D + D \xrightarrow{\sim 50\%} {}^3_2He(0.82\ MeV) + n(2.45\ MeV)$$

$$D + D \xrightarrow{\sim 50\%} {}^3_1H(1.01\ MeV) + H(3.02\ MeV)$$

Secondary Reaction

$$D + {}^3_1H(1.01\ MeV) \rightarrow {}^4_2He(3.5\ MeV + n(14.1\ MeV)$$

MagLIF Hardware

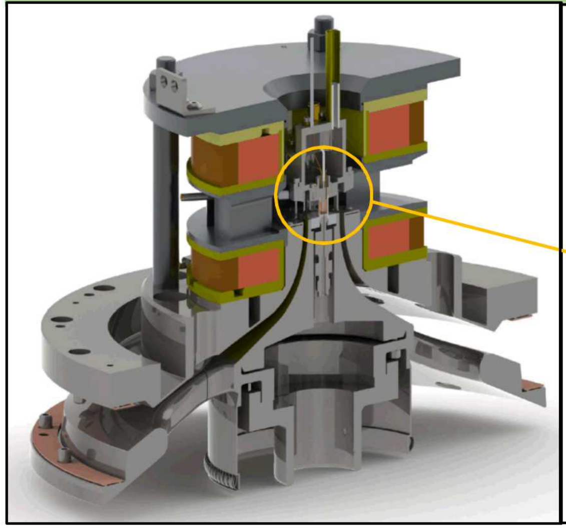

Liner “z-pinch”

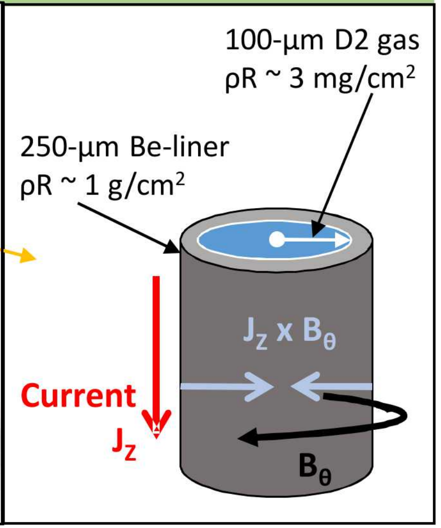

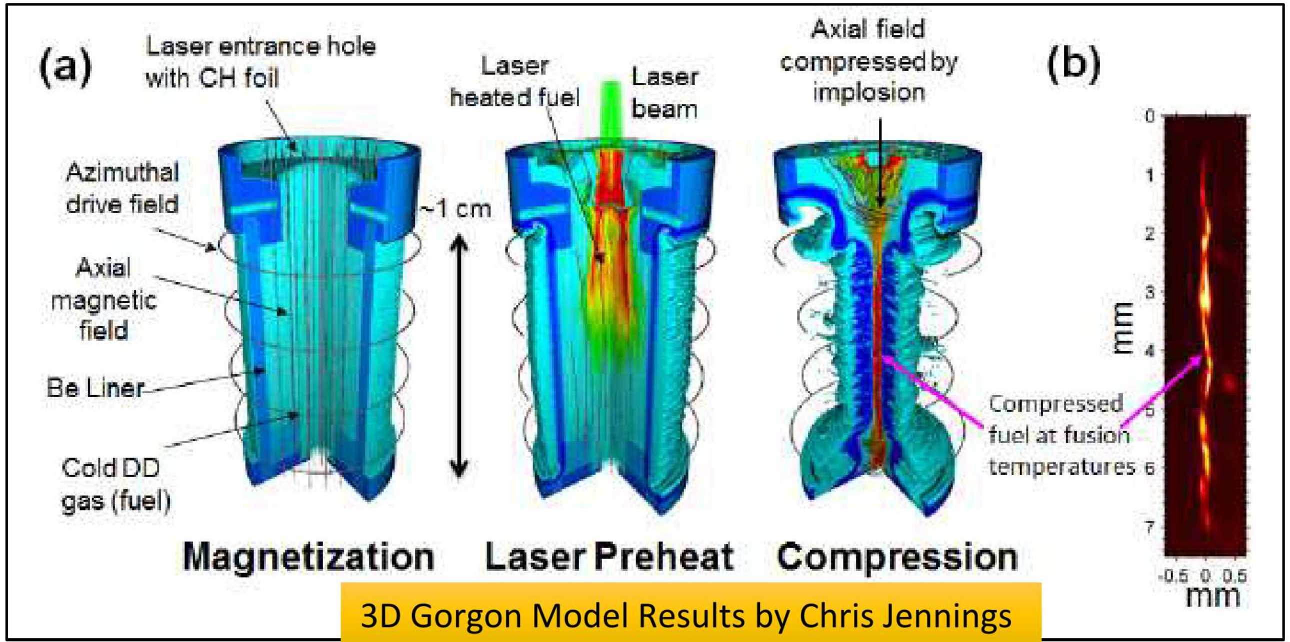

3D Gorgon Model Results by Chris Jennings

There are several diagnostics fielded on MagLIF experiments that view the source through unique geometries.

Cross-section view of the Z-accelerator and diagnostic location

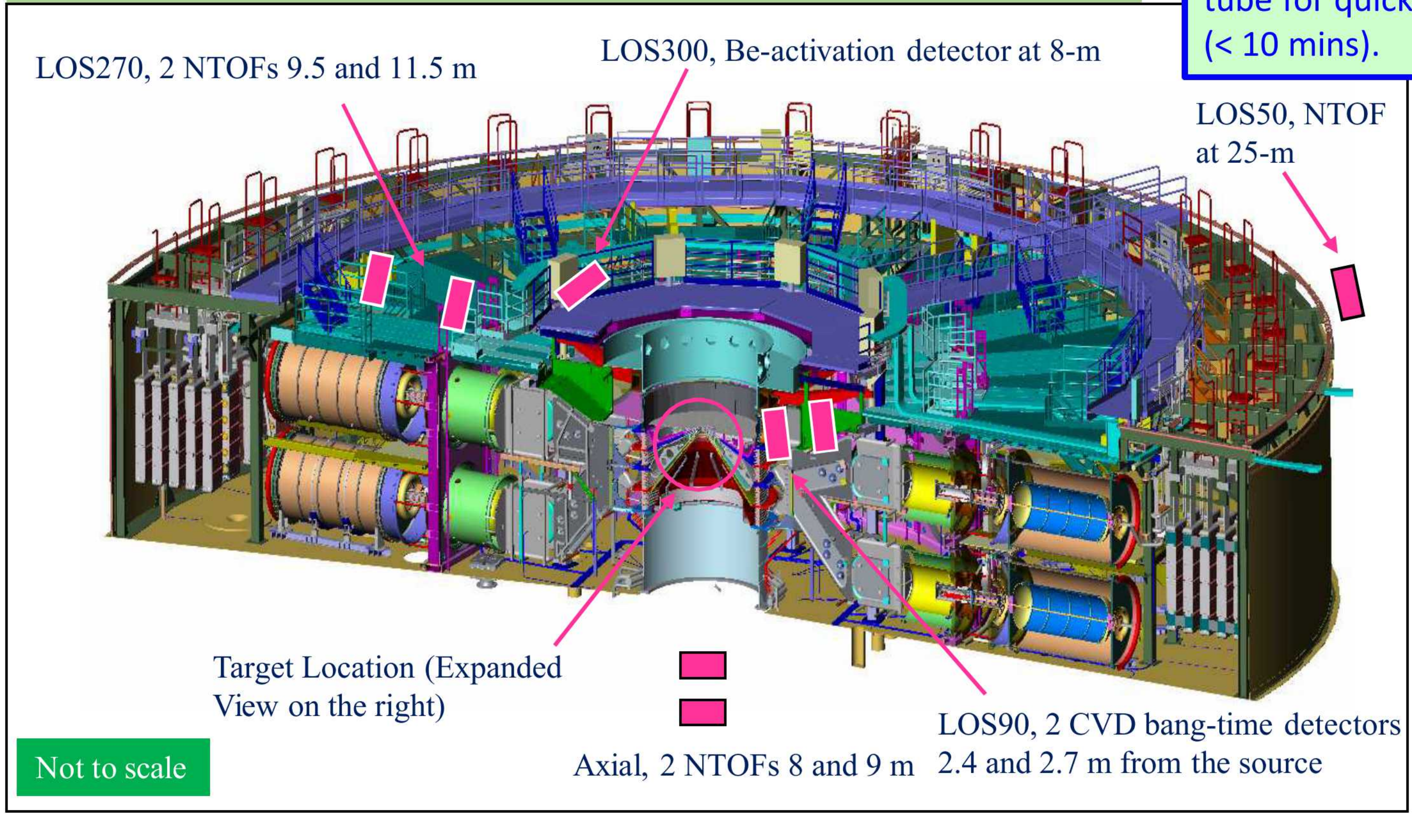

LOS270, 2 NTOFs 9.5 and 11.5 m

LOS300, Be-activation detector at 8-m

LOS50, NTOF at 25-m

Target Location (Expanded View on the right)

Axial, 2 NTOFs 8 and 9 m

LOS90, 2 CVD bang-time detectors 2.4 and 2.7 m from the source

Not to scale

Diagnostics located within the target chamber

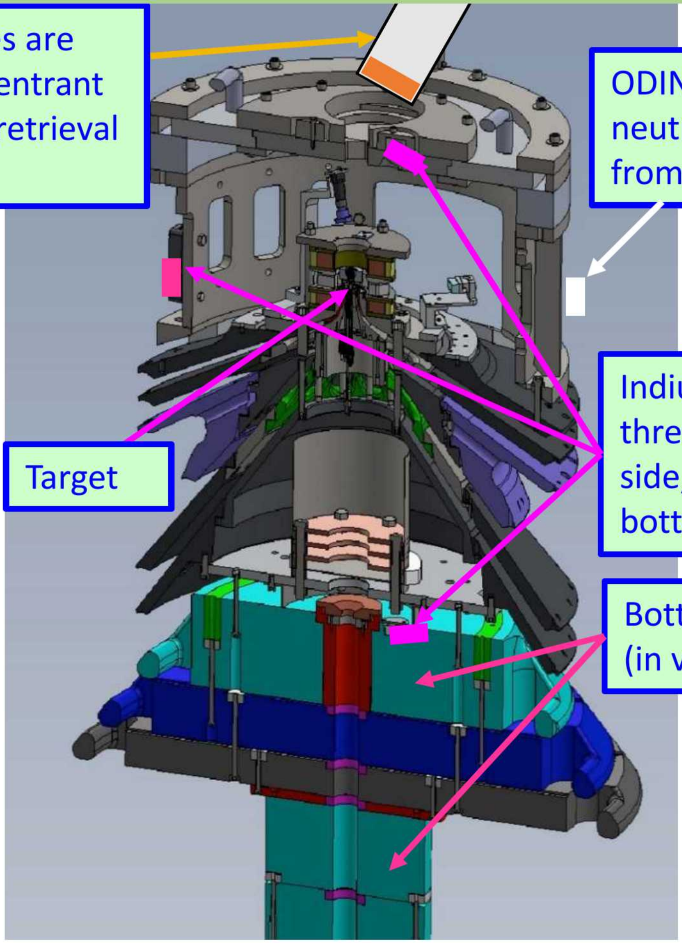

Copper samples are fielded in a re-entrant tube for quick retrieval (< 10 mins).

ODIN (one dimensional neutron imager) ~ 1 m from the source

Target

Indium activation - three top, three side, and three bottom samples

Bottom nTOF collimator (in vacuum)

Information about the reaction kinetics and confinement physics can qualitatively be extracted from the neutron time of flight spectra

H. Brysk, Plasma Phys. **15**, 611 (1973)
C. L. Ruiz et al., Phys. Rev. Lett. **93**, 015001 (2004)
P. F. Schmit et al., Phys. Rev. Lett. **113**, 015001 (2014)
S. B. Hansen et al., Phys. Plasmas **22**, 05613 (2015)
M. R. Gomez et al., Phys Plasmas **22**, 056306 (2015)
P. F. Knapp et al., Phys. Plasmas **22**, 056312 (2015)

CVD Bang-time detectors

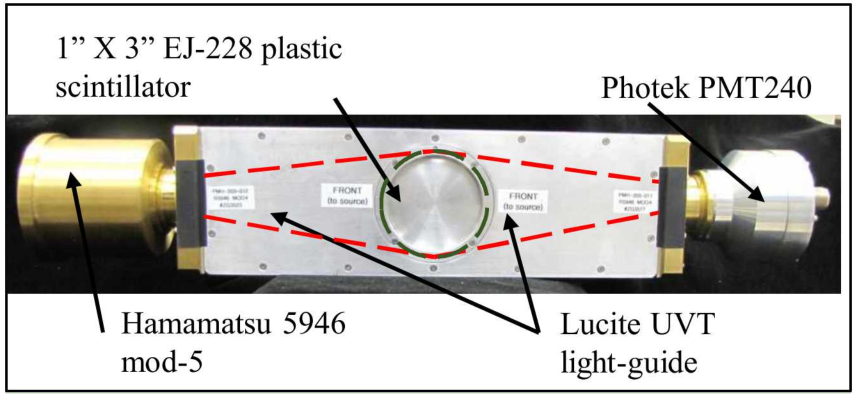

Dual-PMT nToF detector

BR (MG-cm) is the MagLIF confinement parameter inferred from the D-T/D-D yield ratio and the shapes of the D-T axial and radial spectra *Simulated data

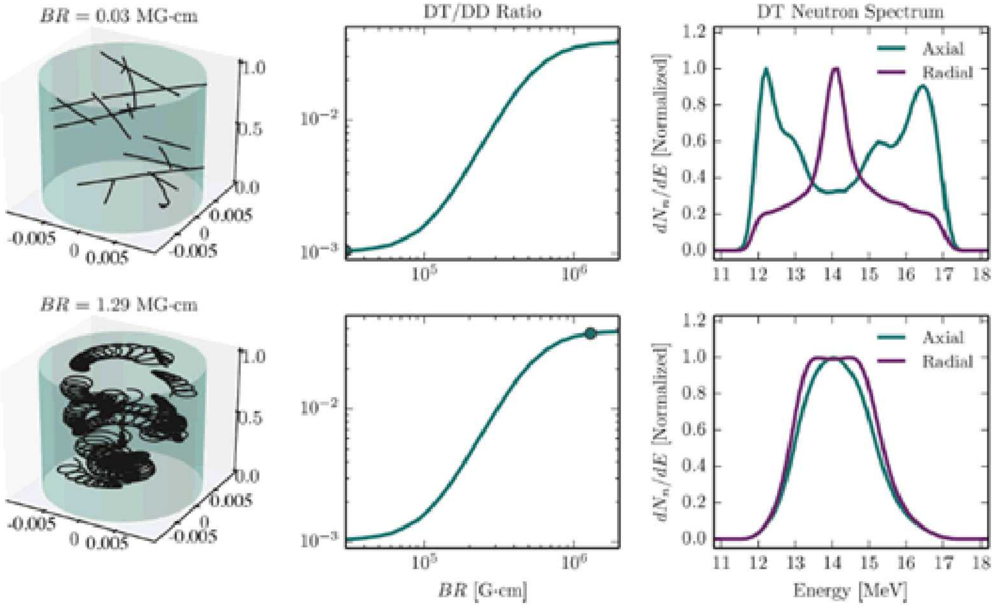

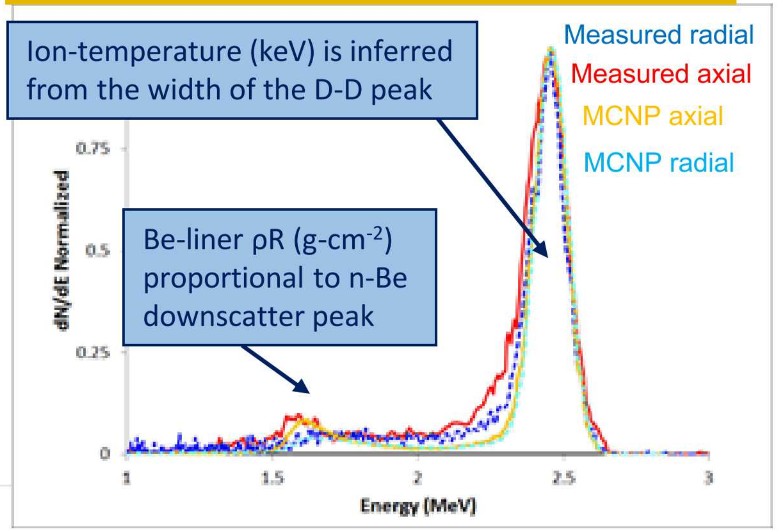

Ion-temperature (keV) is inferred from the width of the D-D peak

Be-liner ρR (g-cm^{-2}) proportional to n-Be downscatter peak

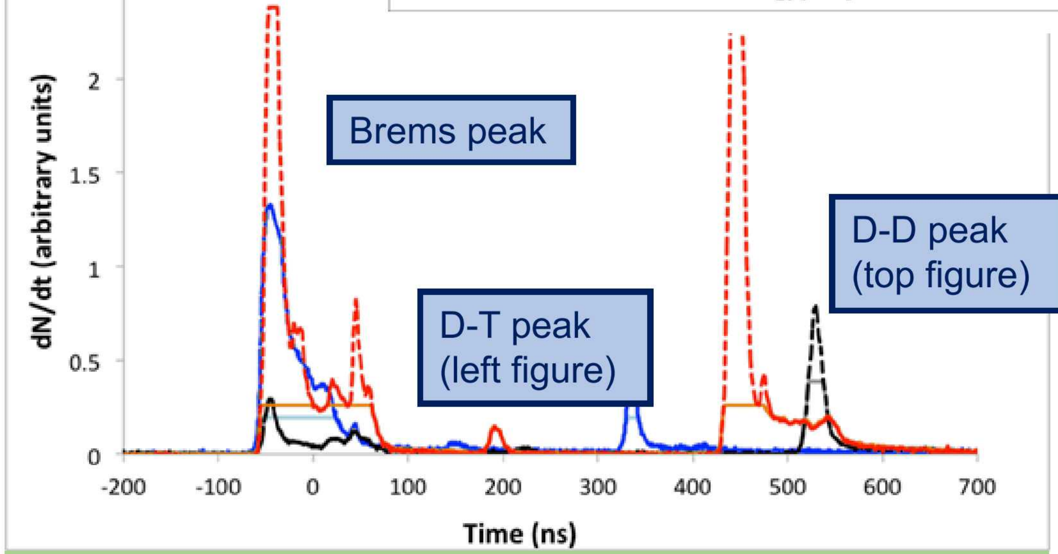

Brems peak

D-T peak
(left figure)

D-D peak
(top figure)

Typical MagLIF nToF spectra at various distances

The neutron producing region within the plasma column can be inferred using ODIN (One dimensional imager of neutrons).

D. Ampleford et al. (accepted by Rev. Sci. Instr. **89** (2018)
J. Vaughan et al. (accepted by Rev. Sci. Instr. **89** (2018)

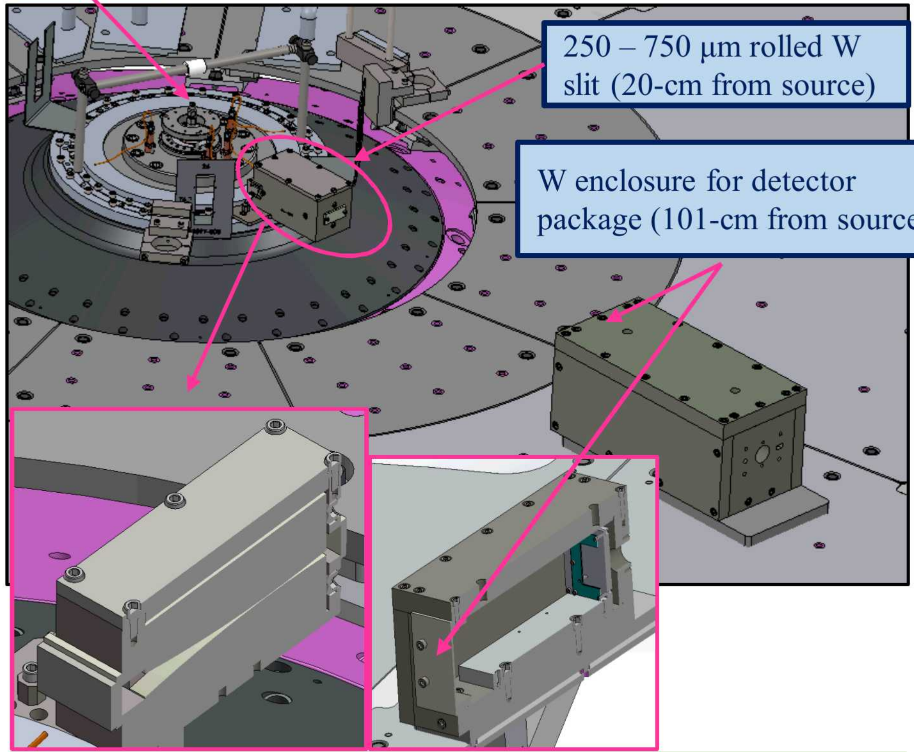

source

250 – 750 μm rolled W slit (20-cm from source)

W enclosure for detector package (101-cm from source)

Diagram of ODIN

ODIN image de-magnified

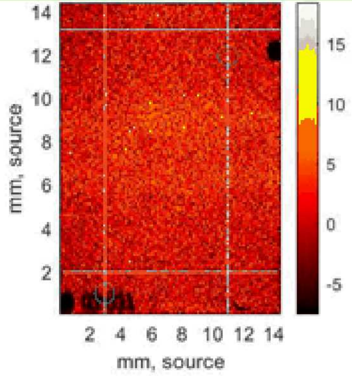

X-ray image of the source

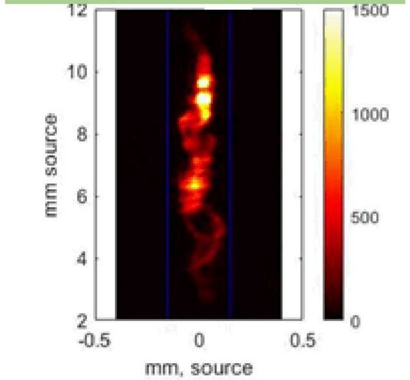

X-ray and ODIN comparison

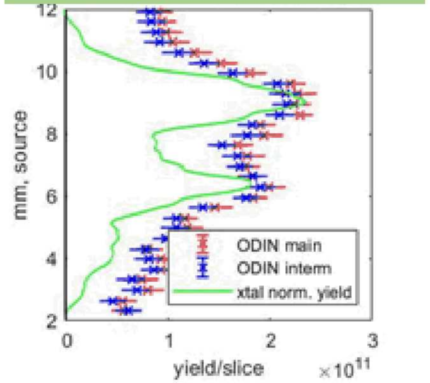

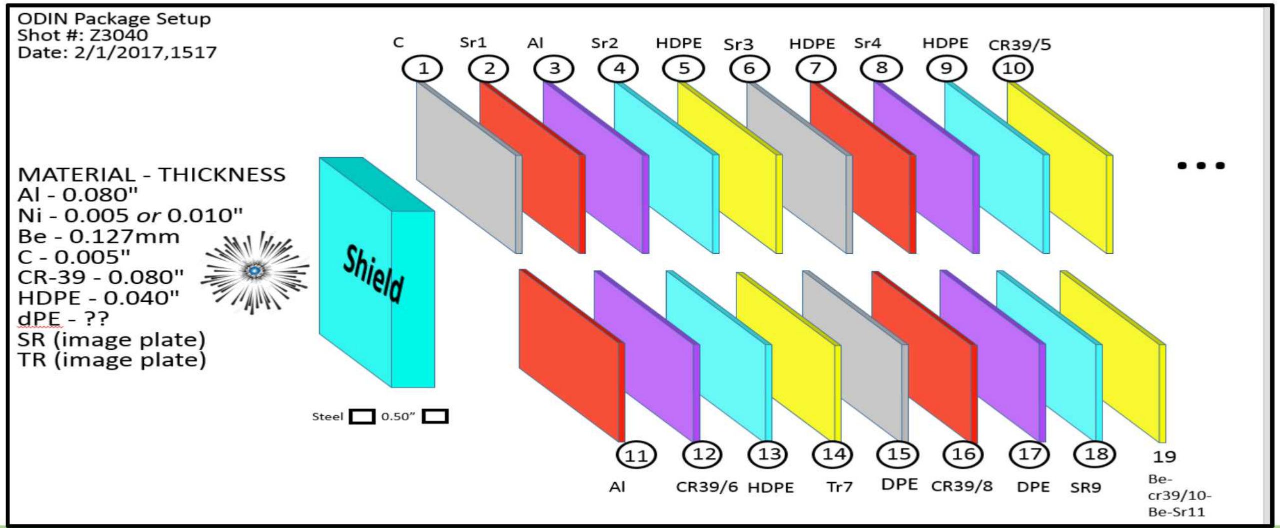

ODIN Package Setup
Shot #: Z3040
Date: 2/1/2017,1517

MATERIAL - THICKNESS
Al - 0.080"
Ni - 0.005 *or* 0.010"
Be - 0.127mm
C - 0.005"
CR-39 - 0.080"
HDPE - 0.040"
dPE - ??
SR (image plate)
TR (image plate)

Typical detector package uses image plate and CR-39 detectors with various radiators